ACS APPLIED MATERIALS & INTERFACES

Research Article

www.acsami.org

High Energy Density and Breakdown Strength from β and γ Phases in Poly(vinylidene fluoride-*co*-bromotrifluoroethylene) Copolymers

Matthew R. Gadinski, Kuo Han, Qi Li, Guangzu Zhang, Wuttiichai Reainthippayasakul, and Qing Wang*

Department of Materials Science and Engineering, The Pennsylvania State University, University Park, Pennsylvania 16802, United States

Supporting Information

ABSTRACT: Poly(vinylidene fluoride) PVDF-based copolymers represent the state of the art dielectric polymers for high energy density capacitors. Past work on these copolymers has been done with limited emphasis on the effects of copolymer composition and with a limited range of defect monomers, focusing primarily on the commercially available poly(vinylidene fluoride-*co*-chlorotrifluoroethylene), P(VDF-CTFE), and poly(vinylidene fluoride-*co*-hexafluoropropylene), P(VDF-HFP), and the processing thereof. To expand on this area of research, copolymers of VDF and bromotrifluoroethylene (BTFE) were synthesized examining the composition range where uniaxial stretching was possible. It is found that P(VDF-BTFE) copolymers with small BTFE contents (< 2 mol %) stabilize the γ phase, compared to P(VDF-CTFE)s and P(VDF-HFP)s that are largely α phase in composition. Furthermore, different from P(VDF-CTFE)s and P(VDF-HFP)s, whose energy storage capabilities depend on the reversibility of the α to β phases transformation, high discharged energy densities (i.e., 20.8 J/cm^3 at 716 MV/m) are also achievable through the β and γ phases in P(VDF-BTFE)s without significantly reducing crystallinity and breakdown strength. This study demonstrates new avenues to the development of high energy density ferroelectric copolymers via manipulation of the γ phase through variation of the structure and content of comonomers.

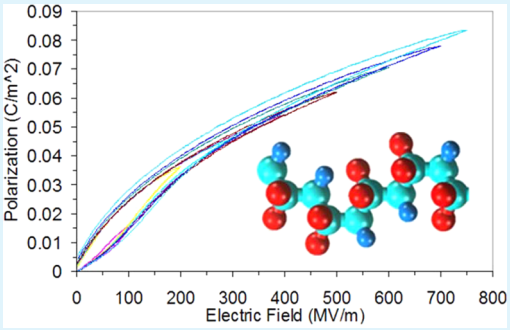

KEYWORDS: *ferroelectric polymers, poly(vinylidene fluoride), dielectric properties, capacitors, energy storage*

1. INTRODUCTION

The development of high energy density dielectric materials for capacitive energy storage holds far-reaching implications in a variety of applications including advanced electronic devices and circuits, pulse power technologies, and electric vehicles.[1] The use of polymeric materials in such applications possesses inherent advantages including lightweight, low cost, ease of processing, self-healing capability, and high breakdown strength.[2] Of these advantages high breakdown strength is the most critical value when considering stored energy density, which for a linear dielectric is expressed in eq 1, where U is stored energy density, k is the dielectric constant, ε_0 is the permittivity of free space, and E is the applied electric field.

$$U = 1/2k\varepsilon_0 E^2 \quad (1)$$

Dielectric polymers, while routinely exhibiting breakdown strengths of ≥300 MV/m, are limited in stored energy density by their low k values (e.g., ∼2−3).[2] For example, the best commercially available polymer dielectric, biaxially oriented polypropylene (BOPP), possessing a breakdown of 730 MV/m and k of 2.2 at 1 kHz, shows an energy density of only ∼4 J/cm^3 at 600 MV/m.[3,4]

This has led to the interest in the poly(vinylidene fluoride), PVDF, for capacitive energy storage due to its relatively high k value (∼10) and breakdown strength (∼590 MV/m).[2,5] While the high k value improves the stored energy density, PVDF is plagued by the large polarization hysteresis resulting from the cooperative polarization of large ferroelectric β-phase domains. The polarization hysteresis leads to significant ferroelectric loss (>50%) and greatly reduced recoverable energy density (∼2.4 J/cm^3 at 590 MV/m).[6] The discharge energy density of PVDF can be improved to ∼10 J/cm^3 at 400 MV/m by processing films into the nonpolar α phase; however, the α phase of PVDF irreversibly transforms into the β phase with application of fields above 400 MV/m.[6] Research into PVDF for capacitor applications has thus focused on reducing the ferroelectric hysteresis and inherent energy loss. In attempts to achieve this goal, PVDF has been defected through copolymerization with bulky comonomers.

For example, copolymers of VDF with trifluoroethylene (TrFE), which were originally developed to enhance the piezoelectric properties of PVDF by stabilizing the ferroelectric β phase, were further modified with the addition of chlorotrifluoroethylene (CTFE), chlorofluoroethylene (CFE), or hexafluoropropylene (HFP).[7,8] The addition of the third bulky comonomer was found to break up the large ferroelectric domains into smaller nanopolar regions dispersed in a nonpolar crystalline phase. This structural modification increased k to

Received: July 23, 2014
Accepted: October 15, 2014
Published: October 16, 2014

>50, while also altering the polarization versus field ($P-E$) behavior from that of a normal ferroelectric to that of a relaxor ferroelectric. Relaxor ferroelectric behavior is characterized by reduced hysteresis and low remnant polarization. While this greatly reduced ferroelectric loss (<25%), the early polarization saturation (occurring at ~250 MV/m) and reduced breakdown (~400 MV/m) also limited energy density to ~10 J/cm^3 at 400 MV/m.[9]

The most successful approach to enhancing the released energy density of PVDF was through direct copolymerization of VDF with only bulky comonomers such as CTFE and HFP. Uniaxially stretched P(VDF-CTFE) and P(VDF-HFP) copolymers exhibit energy densities of 18−25 J/cm^3 at ≥600 MV/m.[10,11] High breakdown strength of P(VDF-HFP) has even led to energy density greater than 25 J/cm^3.[9] While there is only a modest improvement in k, that is, 12 for P(VDF-CTFE) and 16 for P(VDF-HFP) at 1 kHz, with the introduction of these defects, the improvement of breakdown strength, and more importantly, the prevention of polarization saturation, results in very high discharge energy densities.[9] In both of these copolymers, this is accomplished by improving the reversibility of the α to β crystalline phase transformation that occurs irreversibly above 400 MV/m in the homopolymer.[12] In P(VDF-CTFE)s, this occurs through inclusion of the CTFE defect into the crystalline phase stabilizing the α phase, while in P(VDF-HFP)s, exclusion of defect reduces crystallite size limiting the cooperative polarization of large ferroelectric domains. Though the energy densities of P(VDF-CTFE)s and P(VDF-HFP)s are the highest among polymers, there still exists considerable ferroelectric loss due to some remaining irreversible α to β phase transformations.[13,14]

In this paper, we report the study of the copolymers of VDF and bromotrifluoroethylene (BTFE)[15,16] for capacitive energy storage applications. Because of the rapid decrease in crystallinity observed with relatively modest amounts of BTFE defect monomer, it is found that only P(VDF-BTFE) copolymers containing <2 mol % BTFE could be stretched and evaluated.[16] By utilizing only a small amount of defect monomer, the decrease in crystallinity associated with increasing defect concentration is mitigated. Different from the previous examples such as P(VDF-CTFE)s and P(VDF-HFP)s where the high energy density attained depends on improving the reversibility of the α to β phase transformation occurring at fields above 400 MV/m, which is limited as complete reversibility cannot be achieved without compromising the total crystallinity, we demonstrate herein that, through stabilization of the γ phase, high energy density is also achievable without significantly reducing crystallinity. A discharge energy density of 20.8 J/cm^3 and a breakdown strength of 716 MV/m are thus achieved in P(VDF-BTFE)s, which are higher than both P(VDF-CTFE)s and P(VDF-HFP)s given comparable processing conditions.

2. EXPERIMENTAL SECTION

2.1. Synthesis of P(VDF-BTFE) Copolymers. Synthesis of P(VDF-BTFE) copolymers was accomplished via suspension polymerization using a 300 mL stainless steel Parr reaction vessel. 100 mL of deionized water and 0.15 g of potassium peroxodisulfate initiator was added to the vessel, which was subsequently sealed and degassed via vacuum pump and cooled using liquid nitrogen bath. Gaseous VDF and BTFE were pumped into the reaction vessel separately. VDF was pumped in at a rate of 523.6 cm^3/min. BTFE was pumped in at a rate of 385 cm^3/min. The amount of monomer was controlled by varying the time each monomer was allowed to flow into the reaction vessel. VDF was allowed to flow for 17.5, 18.5, and 17.5 min for the homopolymer **PVDF**, **PVB.5**, and **PVB2**, respectively. BTFE was allowed to flow for 0, 7, and 25 s for the homopolymer, **PVB.5**, and **PVB2**, respectively. After charging the vessel with monomer, the vessel was sealed. The vessel was then heated to 90 °C and stirred at 600 rpm for 24 h or until the vessel pressure became stable for 2 h. Once the reaction was complete, the polymer was washed by vacuum filtration with both distilled water and methanol and then dried at 90 °C for 24 h to yield ~15−20 g of white powder corresponded to ~50% conversion. Gel permeation chromatography results using a Viscotek TDA 302 with dimethylformamide (0.01 M LiBr) as eluent at 65 °C with a refractive index detector calibrated by universal calibration with polystyrene standards shows an M_n of ~60 000 g/mol and a polydispersity index of ~1.9.

2.2. Polymer Film Processing. The polymer films were produced via the melt press method. The powder polymers were heated in hydraulic press to 200 °C. Once the desired temperature was achieved, the pressure was increased by 500 psi every 15 min to 6500 psi. The films were left at pressure and temperature for a minimum of 2 h to ensure film uniformity and maximum thinness. The films were then removed from the press and immediately quenched in ice water. Film thicknesses varied between 20 and 30 μm. The films were then stretched over a 150 °C surface to a draw ratio of 5. Film thickness varied between 5 and 15 μm. The originally opaque films became clear after uniaxial stretching. These films were used in all structural characterization and dielectric measurements. For the dielectric measurements, the polymers were sputter-coated with gold using a Denton Vacuum Desk IV sputter coater under an argon atmosphere at 50 mTorr with the instrument setting of 47% power for 125 s. The estimated electrode thickness was 30 nm, and the electrode area was 0.0532 cm^2.

2.3. Characterization. Polymer compositions were determined by ^{19}F NMR. ^{19}F NMR spectra were obtained on Bruker CDPX-300 NMR (300 MHz) equipped with a fluorine probe using a $CFCl_3$ internal standard. Samples were dissolved in deuterated dimethyl sulfoxide and scanned 250 times. The data was acquired using a 11.3 μs pulse width, 1.0 s relaxation delay, 7.4 μs dwell time, 90° flip angle, 67 567.57 Hz spectral window, 0.515 Hz FID resolution, and 0.969 98 s acquisition time. The size of processed data was 65 536, which was set to half that of the total data. The spectral reference frequency was 282.13 MHz. The spectra were processed utilizing no broadening factors and were both phase- and baseline-corrected. Differential scanning calorimetry (DSC) curves were acquired using a TA Instruments model Q 100 DSC and a heating rate of 10 °C/min ramping from 40 to 200 °C. Fourier transform infrared spectroscopy (FTIR) spectra were obtained on a Bruker V70 FTIR using an attenuated total reflectance mode with a Harrick MVP-Pro Star equipped with a diamond prism. Two-dimensional (2-D) XRD spectra were obtained on a Rigaku DMAX RAPID using a fixed geometry and exposing samples for 30 min. The radiation source was a Cu Kα source with a wavelength of 1.54 Å. One-dimensional (1-D) spectra were obtained through integration of the 2-D spectra with respect to 2θ. Peak deconvolution was done using Jade XRD analysis software using either Gaussian or Pearson VII peaks, whichever resulted in the lowest $\langle R^2 \rangle$ value. Complex dielectric constant as a function of frequency at room temperature was analyzed with an Agilent E4980A LCR meter using a 2 V bias. High-field polarization−electric field ($P-E$) loops were measured using a modified Sawyer−Tower circuit with a Trek model 30/20 ± 30 kV high voltage amplifier system. Measurements were performed in Galden HT insulation fluid using a triangular unipolar bias at 10 Hz. The breakdown measurements were performed using the same instrument and setup applying a direct current ramp voltage of 500 V/s until breakdown.

3. RESULTS AND DISCUSSION

3.1. Synthesis and Compositions of P(VDF-BTFE)s. PVDF and P(VDF-BTFE)s with 0.5 and 2.0 mol % BTFE content (designated **PVB.5** and **PVB2**, respectively) were synthesized. Compositions were determined using ^{19}F NMR

with spectra shown in Supporting Information, Figure S1. The main peaks observed in the **PVDF** spectrum are those associated with linking tendencies of the VDF monomer including the normal head to tail (H−T) linkage (head = CF_2, tail = CH_2) (−92.42 to −93.24 ppm) and the T−T (−95.19 ppm) and H−H (−114.30 and −116.56 ppm) defect linkages.[17] The smaller peaks surrounding these main peaks are a result of these linkages in proximity to polymer end groups.[18] Absent in the **PVDF** spectrum are the peaks located at −109.27 and −120.58 seen in the copolymer spectra attributable to the BTFE−BTFE T−H linkages and the BTFE-VDF T−T linkages, respectively.[19] The ratio of VDF to BTFE in the main chain is given by eq 2, which compares integrated peak intensity of the primary linkages of VDF with that of the BTFE containing linkages.

$$\frac{\mathrm{VDF}_{\mathrm{mol\%}}}{\mathrm{BTFE}_{\mathrm{mol\%}}} = \frac{\frac{I_{\mathrm{VDF-VDF,H-T}} + I_{\mathrm{VDF-VDF,T-T}} + I_{\mathrm{VDF-VDF,H-H}}}{2}}{\frac{I_{\mathrm{BTFE-BTFE,T-H}}}{2} + I_{\mathrm{BTFE-VDF,T-T}}} \quad (2)$$

P(VDF-BTFE)s with the BTFE content below 2 mol % were investigated because they are capable of being stretched to a draw ratio of ∼5. Above 2 mol % BTFE, there is found to be a rapid drop in crystallinity and melting temperature, resulting in the films being increasingly brittle.[16] This prevented stretching of P(VDF-BTFE)s with higher BTFE compositions to similar draw ratios. On the other hand, no copolymers of P(VDF-CTFE)s or P(VDF-HFP)s below 4 mol % defect monomer have been examined for high energy density capacitor applications in literature. Though resulting in very high energy densities, the high amount of defect monomer used leads to reductions in either melting temperature or crystallinity of P(VDF-CTFE)s and P(VDF-HFP)s. This study will show that, by utilizing small amounts of defect monomer, high energy density can be achieved in P(VDF-BTFE)s while mitigating the drops in these values.

3.2. Crystallinity. The prepared polymers were uniaxially stretched utilizing a zone-drawing technique at 150 °C of melt pressed and quenched films. While stretching below 90 °C tends to form a predominantly β-phase PVDF, stretching above 120 °C is reported to form oriented α phase.[20] Structural characterization of the stretched films were performed utilizing DSC to determine total crystallinity and melting temperature with 2-D X-ray diffraction (2-D XRD) and FTIR to reveal crystalline orientation and crystalline phase composition.

The DSC plots (see Supporting Information, Figure S2) exhibit two melting endotherms, one small low-temperature peak and a much larger-high temperature peak. The low-temperature peak is attributed to the formation of secondary crystallites formed during room temperature storage, while the high-temperature peak corresponds to the primary crystallization occurring during the stretching procedure.[21] Figure 1 shows the total crystallinity and melting temperature of **PVDF**, **PVB.5**, and **PVB2** as a function of BTFE content, where crystallinity was calculated from $\Delta H^0_{\mathrm{f,PVDF}}$ = 104.7 J/g corresponding to the heat of formation of PVDF with theoretical 100% crystalline.[22] The effect of relatively small amounts of BTFE on crystallinity can be observed in Figure 1 with only 0.5 mol % BTFE resulting in a 5.6% reduction in crystallinity. The crystallinity drops steadily over the composition range from 42.5% crystalline for PVDF to 32.0% at 2 mol % BTFE. The melting temperature is reduced by ∼7 °C from 162 to 155 °C over the same composition range.

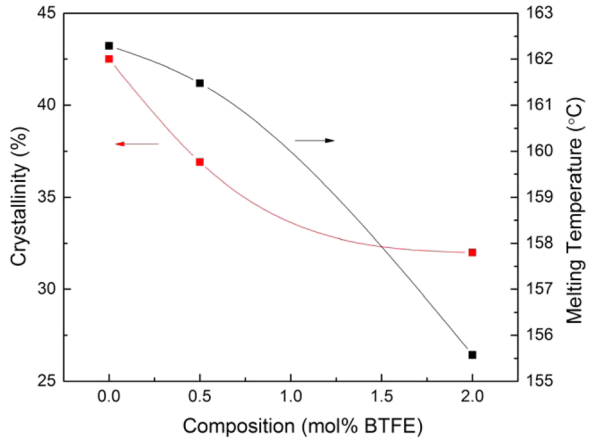

Figure 1. Melting temperature and percent crystallinity as a function of BTFE content.

In comparison, P(VDF-CTFE) with 9 mol % CTFE, which is the commonly researched composition for energy storage capacitors, exhibits a crystallinity < 20%, and comparable melting temperatures to the P(VDF-BTFE)s shown in Figure 1.[11] The P(VDF-HFP) copolymer studied for capacitor applications with a composition of 4 mol % HFP, due to the exclusion of the HFP defects, shows a largely reduced melting temperature to 133 °C, while crystallinity is maintained to similar levels to the P(VDF-BTFE)s.[13] As seen in this comparison, either crystallinity or melting temperature is significantly reduced with addition of the defect monomer in P(VDF-CTFE)s (∼20% drop in crystallinity in comparison to the homopolymer) or P(VDF-HFP) (∼30 °C drop in melting temperature in comparison to homopolymer). By utilizing only small amounts of defect monomer, the decreases in the these values of P(VDF-BTFE) copolymers are considerably less than those previously reported of P(VDF-CTFE)s and P(VDF-HFP)s.

3.3. Crystallite Orientation and Structures. 2-D XRD was utilized to examine the crystalline phase in terms of phase composition and orientation. Figure 2 presents the 2-D diffraction rings for **PVDF** (Figure 2a), **PVB.5** (Figure 2b), and **PVB2** (Figure 2c). In all samples, the most intense peak is at 20.3° 2θ ascribed to (110/200) β phase, which is located on the equatorial plane, indicating a perpendicular orientation to the chain direction for these lateral crystallite planes.[13] At 17.7° and 18.4° 2θ are the (100) and (020) α phase reflections, respectively, which are best seen by looking at the 1-D spectra (Figure 2d) determined from 2-D data by integrating the intensity versus 2θ.[13] These peaks were used to quantify the orientation of the crystallites in terms of Herman's orientation parameter, described by eq 3, where f is Herman's orientation parameter, $\langle \cos^2(\phi) \rangle$ is the average angle between a crystalline reflection and a reference angle (stretch direction) (eq 4), and I_{hkl} is the intensity of a given crystalline reflection as a function of ϕ.[23]

$$f = \frac{3\langle \cos^2(\phi) \rangle - 1}{2} \quad (3)$$

$$\left\langle \cos^2(\phi) \right\rangle = \frac{\int_0^{\pi} I_{hkl}(\phi) \cos^2(\phi) \sin(\phi) \mathrm{d}\phi}{\int_0^{\pi} I_{hkl}(\phi) \sin(\phi) \mathrm{d}\phi} \quad (4)$$

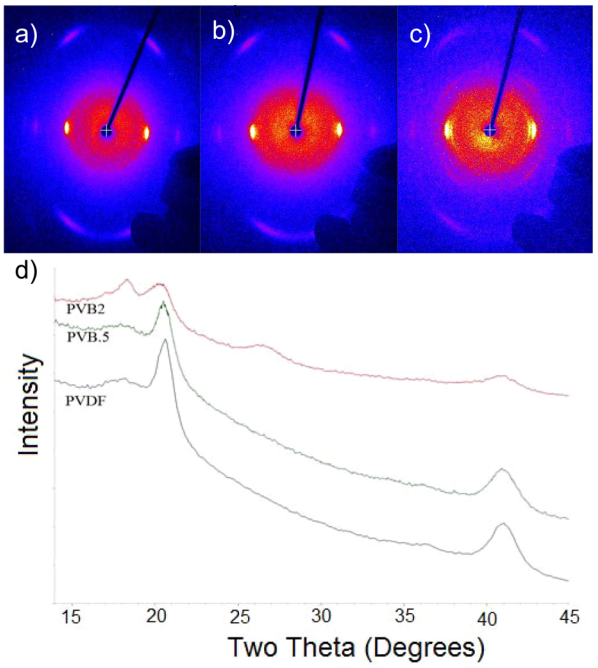

Figure 2. 2-D X-ray diffraction rings of (a) **PVDF**, (b) **PVB.5**, and (c) **PVB2**. (d) 1-D spectra determined from integration of diffraction rings as a function of 2θ. (1-D spectra are offset for clarity; peaks at 17.7°, 18.4°, 19.9°, 26.5°, and 41.6° 2θ correspond to the (100), (020), (110), (021), and (211) planes of both the α and γ phases; the peak at 20.3° 2θ corresponds to the (110/200) planes of the β phase).

Depending on orientation, f can possess values from 1 to −0.5 where values 1, 0, and −0.5 are indicative of parallel, random, and perpendicular orientation, respectively.[23] The I versus ϕ curves for (110/200) β and (100), (020) α phase reflections can be found in Supporting Information, Figures S3 and S4, respectively. To characterize only the crystallite orientation, the amorphous contribution was removed from the curves by eliminating the baseline. The β phase was found to be oriented to similar degrees with values of −0.409, −0.398, and −0.400 for **PVDF**, **PVB.5**, and **PVB2**, respectively. The α crystallites in the **PVDF** sample were found to have only a minor amount of orientation with a value of only −0.087, while the copolymers exhibited higher values of −0.311 and −0.288 for **PVB.5** and **PVB2**, respectively. This higher degree of orientation of the α crystallites in the P(VDF-BTFE)s could be a result of the reduced secondary crystallization as indicated in Supporting Information, Figure S2 with the low-temperature peaks shifting to lower temperatures and decreasing in intensities. As all of the degrees of orientation are found to be similar between the samples, any difference in terms of crystalline phase composition or crystalline dimensions must then arise from the differences in defect monomer content and not processing.

Figure 3 summarizes the phase composition (Figure 3a), lattice spacings (Figure 3b), and crystallite sizes (Figure 3c) determined from the fits to the 1-D XRD spectra. The amorphous content is seen in Figure 3a to match the crystallinity determined from DSC exactly. The β phase is found to be the major crystalline phase for the stretched **PVDF** and **PVB.5** with the α/γ phase dominating in **PVB2**. Both the α and γ phases share the same characteristic peaks and cannot be differentiated from XRD.[24] This will be further discussed in the FTIR data below. For P(VDF-CTFE)s and P(VDF-HFP)s, the

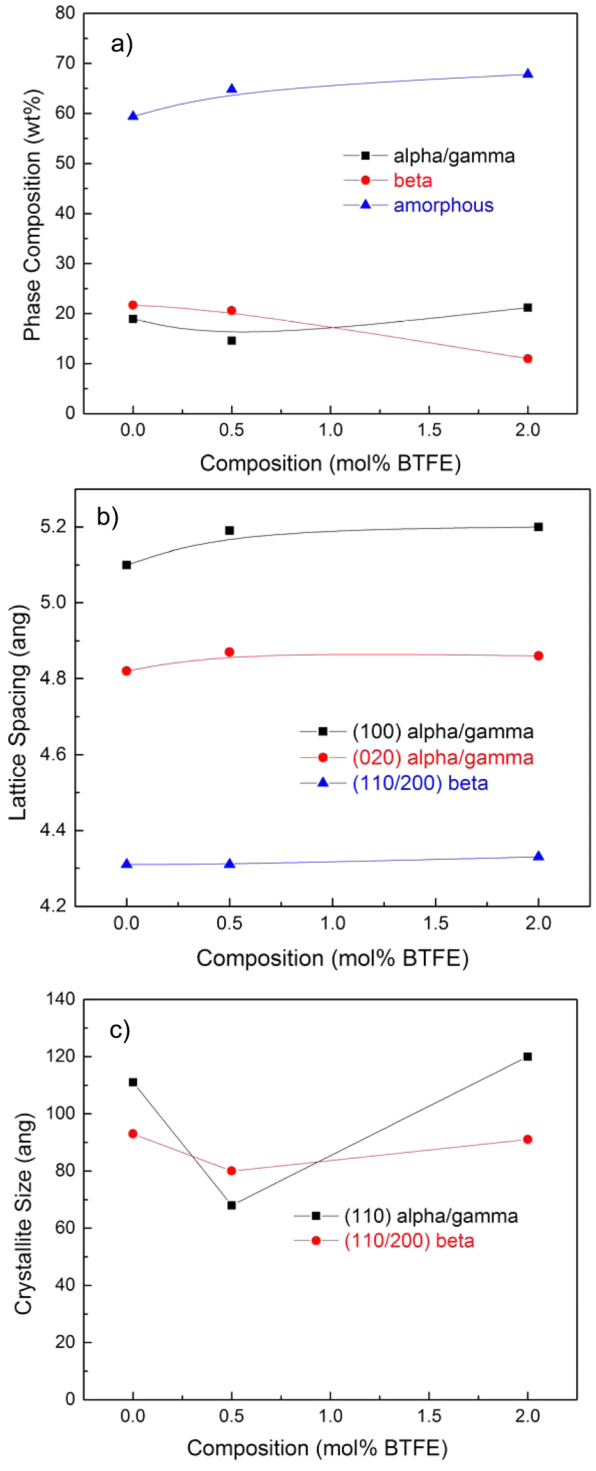

Figure 3. (a) Phase composition, (b) lattice spacing, and (c) crystallite size determined from 1-D XRD spectra fits. (Phase composition determined from peak area, lattice spacing calculated from Bragg's law, and crystallite size determined from the Scherrer Equation).

α phase is the dominant phase due to the destabilization of the β phase. This begins to happen also in the P(VDF-BTFE) copolymers and can be seen approaching 2 mol % BTFE. Complete destabilization of the β phase, however, does not occur until 5 mol % BTFE.[16]

The expansion of the lateral lattice spacing of the (100) and (020) α-phase peaks shown in Figure 3b indicates that the BTFE defect is included exclusively into this phase as the β-

phase lattice spacing stays constant across the composition range.[10] In terms of crystallite size, Figure 3c shows there is a modest decrease in the β crystallites in comparing the P(VDF-BTFE) copolymers to the **PVDF** homopolymer. The α phase in **PVB.5**, however, shows a substantial decrease in crystallite size compared to the homopolymer, while the crystallite size of this phase increases as it becomes the dominant phase in **PVB2**. With crystallite sizes of both phases in **PVB.5** being below 100 Å, this copolymer exhibits even smaller crystallite sizes than P(VDF-HFP)s, suggesting that it should possess a further reduction in ferroelectric domain coupling.[12]

As discussed above, the α and γ phases cannot be distinguished from XRD due to the overlapping of their characteristics peaks. FTIR was then utilized to further elucidate the content of these phases in the polymers. This, however, can only provide a relative content of these phases as the amorphous contribution to the peaks cannot be separated from the crystalline contributions. Figure 4a shows the FTIR spectrum of **PVDF**, **PVB.5**, and **PVB2**. The PVDF spectra (Figure 4a) shows characteristic peaks of the α phase located at 408, 532, 614, 764, 796, 976, and 1219 cm^{-1}.[20,24−26] The peaks associated with the β phase are located at 445 and 1275 cm^{-1}, and peaks attributed to the γ phase are located at 430 and 1235 cm^{-1}.[20,24−26] In **PVB.5**, all peaks associated with α phase are found to be significantly reduced with concurrent increases in both the β and γ phase peaks along with the peaks located at 840 and 512 cm^{-1} attributable to both the β and γ phases.[20,24−26] **PVB2** exhibits a re-emergence of the α-phase peaks with increased BTFE content. Peaks commonly used to characterize the three phases are those located at 1275, 1235, and 1219 cm^{-1}. This region is highlighted in Supporting Information, Figure S5. Significant in this figure is the absence of the 1219 cm^{-1} α-phase peak in **PVB.5** and concurrent increases in the intensity of the β- and γ-phase peaks.

To quantify these changes, the intensity of the peaks located at 430, 408, and 445 cm^{-1} were compared as they are related to the TTTG, TG, and all-trans (T-trans, G-gauche) chain conformations, respectively.[20,24−26] The spectra between 460 and 400 cm^{-1} showing these peaks can be found in Figure S6 of the Supporting Information. These conformations are characteristic of the γ, α, and β crystalline phases, respectively.

Figure 4b displays the distribution of the chain conformations across the composition range. Again it must be stated that the conformation distribution contains both the crystalline and amorphous contributions, requiring the XRD data to be considered when interpreting them. The **PVDF** sample is found to be dominated by the all-trans conformation expected as a result of the uniaxial stretching and the majority phase being the β phase. The XRD also indicates a significant α- or γ-phase content in the **PVDF** sample as indicated by Figure 3a. The FTIR indicates approximately equal amounts of the TG and TTTG conformations indicative of these phases. Because of the amorphous contribution it is impossible to determine the exact amount of each phase, but it is reasonable to assume that some amount of each phase is present.

The **PVB.5** sample shows a substantial increase in the all-trans conformation and a corresponding drop in the TG content. Comparing with the XRD data there is found to be almost no change in the β-phase content and a slight decrease in the α- or γ-phase content. Since there is no increase in the β-phase content from XRD, the increase in the all-trans conformation must then be a result of an increase of this conformation in the amorphous phase. The significant drop in

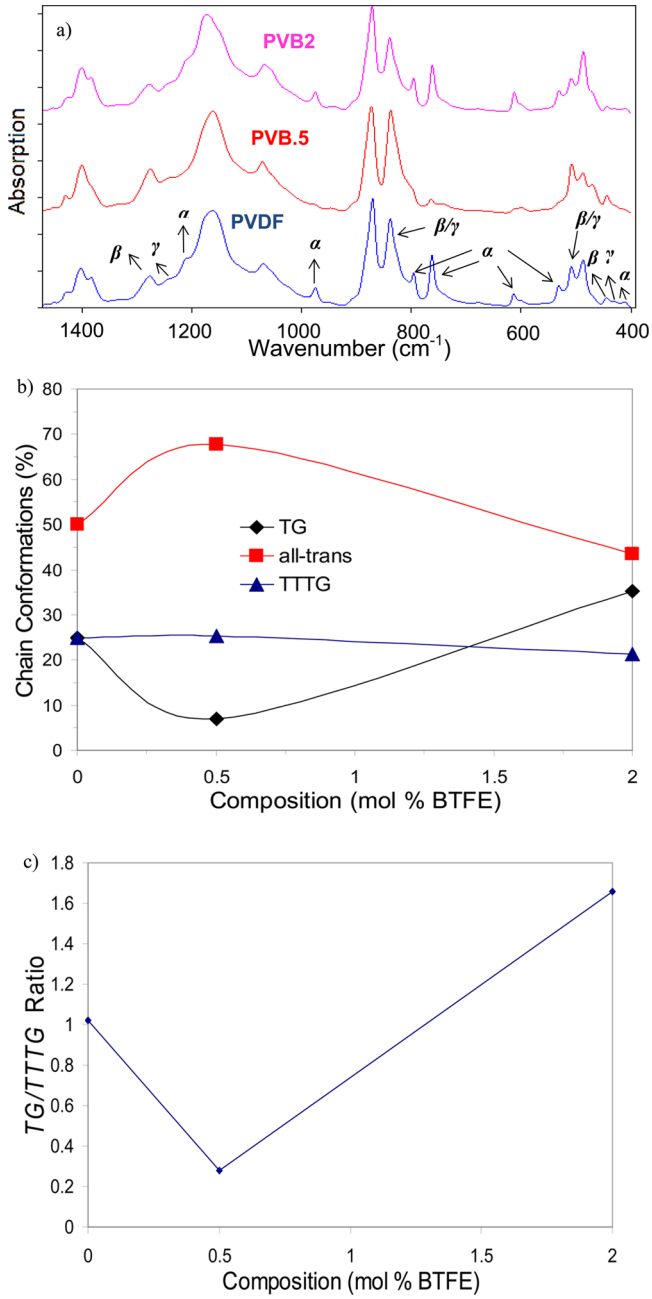

Figure 4. (a) FTIR spectra of PVDF and P(VDF-BTFE) copolymer (b) Percentage of chain conformation as a function of composition (c) and α/γ phase ratio.

the TG conformation must then indicate that the α/γ phase from the XRD is dominated by the γ phase as the TG conformation only accounts for ~7% of the total chain conformations, while the α/γ phase from the XRD is still 14.6% of the total phase content.

Finally, the **PVB2** sample shows a significant reduction in the all-trans conformation, which is consistent with the decrease in the β-phase content from the XRD analysis. Concurrent is the re-emergence of the α-phase peaks in FTIR, the increase in the TG chain conformation, and the α phase becoming the dominant crystalline phase indicated by the XRD. Increasing the BTFE content is found to stabilize the α phase at sufficient content, which mirrors the effect observed in P(VDF-CTFE)s.[10]

Figure 4c shows the ratio of the TG conformation to that of the TTTG as a function of BTFE content. This ratio shows drastic changes with increasing BTFE content. At 0.5 mol % BTFE the ratio is found to decrease from ~1 in **PVDF** to 0.28 indicative of higher γ-phase content than α phase. At 2 mol % BTFE the ratio increases to 1.66, which indicates higher α-phase content and is supported by the α phase being the dominant phase in XRD.

3.4. Dielectric Spectra. Figure 5 presents the weak-field dielectric spectra of **PVDF** and P(VDF-BTFE) copolymers as a function of frequency measured at room temperature. Stretching reduces ionic conduction, which is shown by the flat response in the loss tangent at low frequencies.[27] All polymers show relatively low dielectric loss tangents with values of 0.021, 0.025, and 0.028 for **PVDF**, **PVB.5**, and **PVB2**, respectively, at 1 kHz and increases with increasing amorphous content. **PVB.5** possesses the highest permittivity of 12.8 at 1 kHz compared with values of 10.5 and 10.0 for **PVDF** and **PVB2**, respectively, at the same frequency. The high permittivity of **PVB.5** can be explained by being comprised of >93% polar chain conformations and possessing high amounts of both β and γ polar crystalline phases with small crystallite sizes. The reduction in permittivity for **PVB2** is a result of the increased amount of α-phase content and reduction in crystallinity.

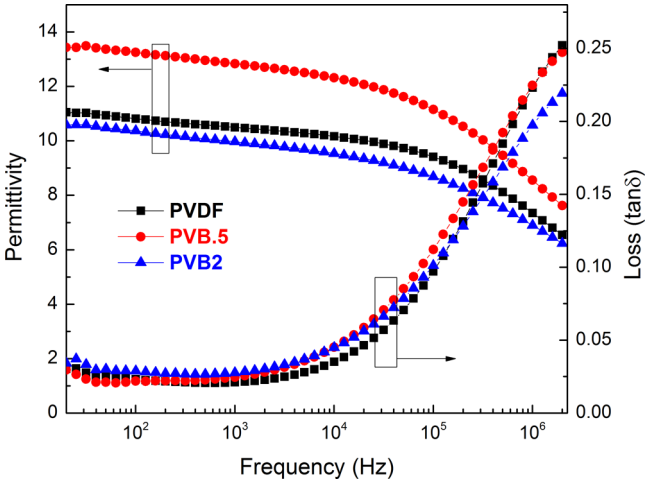

Figure 5. Dielectric spectra as a function of frequency of **PVDF**, **PVB.5**, and **PVB2** measured at room temperature.

3.5. Energy Storage Properties. The high-field performance was evaluated in terms of unipolar P/E loops, which can be found in Supporting Information, Figures S7a, S8a, and S9a, and with the conduction contribution to the loops removed in Supporting Information, Figures S7b, S8b, and S9b. The equations and method for conduction subtraction is listed in Equations S1−S3 in Supporting Information. Figure 6 shows the discharge energy densities of **PVDF**, **PVB.5**, and **PVB2** deduced from the unipolar P/E loops with conduction removed. **PVB.5** exhibits the highest energy density of the evaluated polymers possessing a value of 20.8 J/cm^3 (20.5 J/cm^3 with conduction) at 750 MV/m. In comparison, **PVDF** and **PVB2** have discharge energy densities of 13.3 (13.0 J/cm^3 with conduction) and 13.8 J/cm^3 (13.6 J/cm^3 with conduction) at 600 MV/m, respectively.

Though P(VDF-CTFE)s and P(VDF-HFP)s have been reported to exhibit energy densities of 25.0 J/cm^3, this is only achieved when the samples have been blow-extruded prior to uniaxial stretching. When melt pressed and stretched, P(VDF-CTFE)s and P(VDF-HFP)s exhibit energy densities of 17.0 J/cm^3 and 13.5 J/cm^3 at ~550 MV/m, respectively, which are lower than the 20.8 J/cm^3 achieved by **PVB.5**.[10,13] Because of the laboratory-scale reaction used to produce P(VDF-BTFE) copolymers at tens of grams scales, extrusion typically requiring ~kg of polymer was not possible, but given improved processing conditions, the properties of P(VDF-BTFE) copolymers would also likely be increased.

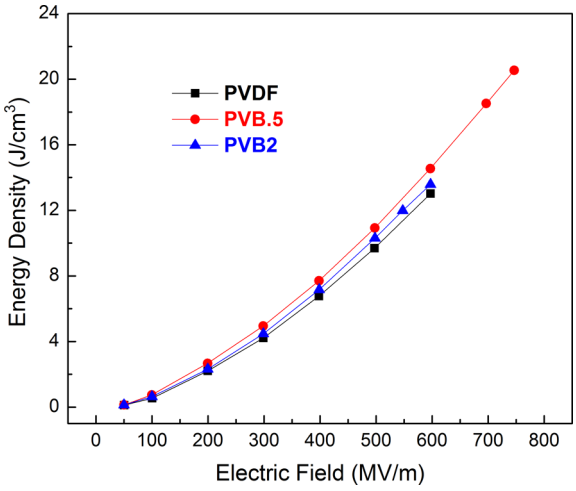

Figure 6. Discharge energy density of **PVDF**, **PVB.5**, and **PVB2** as a function of applied field.

PVB.5 was shown by P/E loop measurements to also withstand high applied fields of >700 MV/m. Weibull breakdown measurements were performed to determine the breakdown strength of the **PVDF**, **PVB.5**, and **PVB2** samples and are summarized in Figure 7 with the α value representing the breakdown field where 63.2% of samples fail and the β shape factor characterizing the spread in the distribution. The stretched **PVDF** exhibits a breakdown value of 565 MV/m, which is comparable to the literature value of 590 MV/m.[9] The breakdown strength of **PVB2** shows a slight reduction to 535 MV/m in comparison to **PVDF**. This is likely a result of the decreased crystallinity of the sample. **PVB.5** on the other hand exhibits a Weibull breakdown value of 716 MV/m and high β value of 9.8. The high breakdown strength of **PVB.5** is likely related to the high γ-phase content of this sample, this being the most significant difference between **PVB.5** and the other samples. Homopolymer samples containing high γ-phase content have previously been shown to possess superior breakdown strength in comparison to those processed into either the β or α phases by preventing polarization saturation and phase transformations below 600 MV/m.[6]

The breakdown strength of **PVB.5** is also higher than both P(VDF-CTFE)s and P(VDF-HFP)s even given blown extrusion and stretching processing. The best reported values of these copolymers is 620 MV/m and 700 MV/m for P(VDF-CTFE)s and P(VDF-HFP)s, respectively.[11]

4. CONCLUSIONS

The copolymers of VDF and BTFE with > 2 mol % BTFE were prepared and then melt-pressed and uniaxially stretched to determine the viability of these copolymers for high energy density capacitor applications. It was found that, by utilizing only a small amount of defect monomer, the reduction in

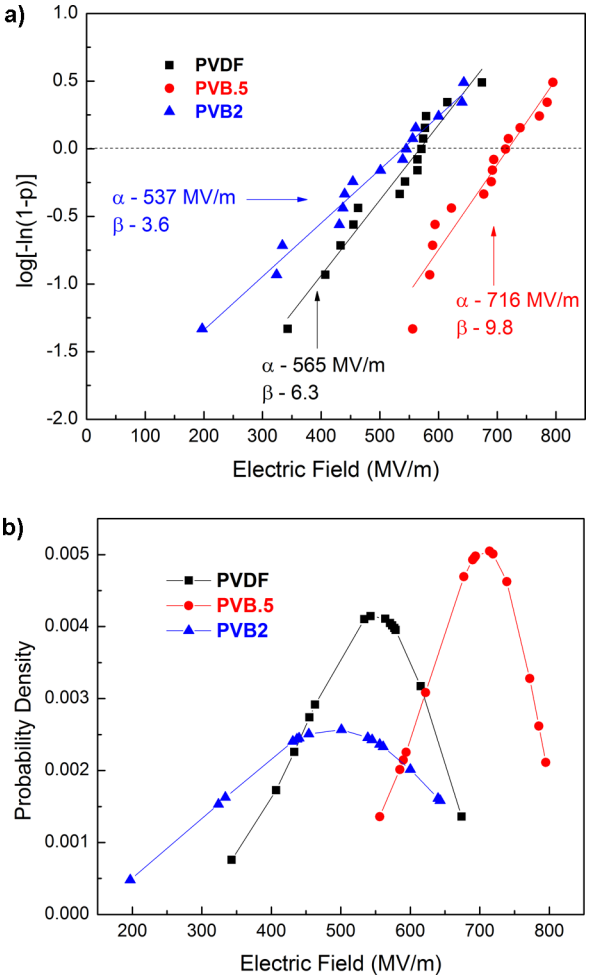

Figure 7. (a) Weibull breakdown plot of **PVDF**, **PVB.5**, and **PVB2**. (b) Accumulated probability of failure as a function of applied electric fields.

crystallinity or melting temperature associated with increasing defect concentration was minimized. In terms of phase, the polymers were found to be comprised of mixed crystalline phase of highly oriented β phases and slightly less oriented α/γ phase. FTIR analysis indicated that the α/γ phase from XRD was largely comprised of γ phase with small amounts of BTFE but became increasingly α phase with increases in BTFE content. This shows a different phase composition than previously reported PVDF-based copolymers where the α phase is the dominant crystalline phase. **PVB.5** dominated by β and γ phases and small crystallite sizes exhibited the best high-field performance with a discharge energy density of 20.8 J/cm^3 at 750 MV/m, and a Weibull breakdown strength of 716 MV/m. The discharge energy density of **PVB.5** is higher than either P(VDF-CTFE) or P(VDF-HFP) given similar processing conditions, and exhibits higher breakdown strength than the best reported values for these copolymers. Considering the large improvement in the properties of P(VDF-CTFE)s and P(VDF-HFP)s received from improved processing conditions, that is, blow extrusion, the electrical energy storage properties of P(VDF-BTFE)s could also be further improved.

While the energy storage capabilities of both the α- and β-phase PVDF-based ferroelectric polymers have been largely explored, the γ phase is rarely discussed. This study demonstrates the viability of this phase for high energy density capacitor materials, which also requires substantially less defect monomer. In comparison, the stabilization of the α phase requires far greater amounts of defect monomer resulting in largely reduced crystallinity or melting temperature in turn reducing breakdown strength. Further optimization of the γ-phase content through either a different defect species or content may then lead to energy densities > 25 J/cm^3, which have thus far proved elusive in PVDF-based ferroelectric polymers.

■ ASSOCIATED CONTENT

Ⓢ Supporting Information

^{19}F NMR spectra, melting endotherms, intensity versus Φ plots, FTIR spectra of peaks between 400 and 480 cm^{-1} and between 1180 and 1300 cm^{-1}, and polarization versus field loops of **PVDF**, **PVB.5**, and **PVB2** before and after conduction subtraction. This material is available free of charge via the Internet at http://pubs.acs.org.

■ AUTHOR INFORMATION

Corresponding Author

*E-mail: wang@matse.psu.edu.

Notes

The authors declare no competing financial interest.

■ ACKNOWLEDGMENTS

This work was supported by Dow Chemical Company and the Office of Naval Research.

■ REFERENCES

(1) Sarjeant, W. J.; Zirnheld, J.; MacDougall, F. W.; Bowers, J. S.; Clark, N.; Clelland, I. W.; Price, R. A. In *Handbook of Low and High Dielectric Constant Materials and Their Applications;* Nalwa, H., Ed.; Academic Press: New York, NY, 1999; Vol. 2, Chapter 9, pp 423−491.

(2) Zhu, L.; Wang, Q. Novel Ferroelectric Polymers for High Energy Density and Low Loss Dielectrics. *Macromolecules* **2012**, *45*, 2937−2954.

(3) Rabuffi, M.; Picci, G. Status Quo and Future Prospects for Metallized Polypropylene Energy Storage Capacitors. *IEEE Trans. Plasma Sci.* **2002**, *30*, 1939−1942.

(4) Michalczyk, P.; Bramoulle, M. Ultimate Properties of the Polypropylene Film for Energy Storage Capacitors. *IEEE Trans. Magn.* **2003**, *39*, 362−365.

(5) Lovinger, A. Ferroelectric Polymers. *Science* **1983**, *220*, 1115−1121.

(6) Li, J.; Meng, Q.; Li, W.; Zhang, Z. Influence of Crystalline Properties on the Dielectric and Energy Storage Properties of Poly(vinylidene fluoride). *J. Appl. Polym. Sci.* **2011**, *122*, 1659−1668.

(7) Furukawa, T. Structure and Functional Properties of Ferroelectric Polymers. *Adv. Colloid Interface Sci.* **1997**, *71−72*, 183−208.

(8) Lu, Y.; Claude, J.; Neese, B.; Zhang, Q.; Wang, Q. A Modular Approach to Ferroelectric Polymers with Chemically Tunable Curie Temperatures and Dielectric Constants. *J. Am. Chem. Soc.* **2006**, *128*, 8120−8121.

(9) Wang, Y.; Zhou, X.; Chen, Q.; Chu, B.; Zhang, Q. Recent Development of High Energy Density Polymers for Dielectric Capacitors. *IEEE Trans. Dielectr. Electr. Insul.* **2010**, *17*, 1036−1042.

(10) Chu, B.; Zhou, X.; Ren, K.; Neese, B.; Lin, M.; Wang, Q.; Bauer, F.; Zhang, Q. A Dielectric Polymer with High Electric Energy Density and Fast Discharge Speed. *Science* **2006**, *313*, 334−336.

(11) Zhou, X.; Chu, B.; Neese, B.; Lin, M.; Zhang, Q. Electrical Energy Density and Discharge Characteristics of a Poly(vinylidene fluoride-chlorotrifluoroethylene) Copolymer. *IEEE Trans. Dielectr. Electr. Insul.* **2007**, *14*, 1133−1138.

(12) Ranjan, V.; Yu, L.; Nardelli, M. B.; Bernholc, J. Phase Equilibria in High Energy Density PVDF-Based Polymers. *Phys. Rev. Lett.* **2007**, *99*, 047801.
(13) Guan, F.; Wang, J.; Pan, J.; Wang, Q.; Zhu, L. Effects of Polymorphism and Crystallite Size on Dipole Reorientation in Poly(vinylidene fluoride) and Its Random Copolymers. *Macromolecules* **2010**, *43*, 6739−6748.
(14) Khanchaitit, P.; Han, K.; Gadinski, M. R.; Wang, Q. Ferroelectric Polymer Networks with High Energy Density and Improved Discharged Efficiency for Dielectric Energy Storage. *Nat. Commun.* **2013**, *4*, 2845 doi: 10.1038/ncomms3845.
(15) Moggi, G.; Bonardelli, P. Copolymers of 1,1-Difluoroethene with Tetrafluoroethene, Chlorotrifluoroethene, and Bromotrifluoroethene. *J. Polym. Sci.* **1984**, *22*, 357−365.
(16) Gadinski, M.; Chanthad, C.; Dong, L.; Wang, Q. Synthesis of Poly(vinylidene fluoride-co-bromotrifluoroethylene) and Effects of Molecular Defects on Microstructure and Dielectric Properties. *Polym. Chem.* **2014**, *5*, 5957−5966.
(17) Wormald, P.; Ameduri, B.; Harris, R. K.; Hazendonk, P. High-resolution ^{19}F and ^{1}H NMR of Vinylidenefluoride Telomer. *Polymer* **2008**, *49*, 3629−3638.
(18) Pianca, M.; Barchiesi, E.; Giuseppe, E.; Radice, S. End Groups in Fluoropolymers. *J. Fluorine Chem.* **1999**, *95*, 71−84.
(19) Murasheva, Y. M.; Shaskov, A. S.; Galil-Ogly, F. A. Analysis of ^{19}F NMR Spectra of Vinylidene Fluoride-Trifluorochloroethylene Copolymers. *Polym. Sci. U.S.S.R.* **1980**, *21*, 968−974.
(20) Gregorio, R. Determination of the α, β, and γ Crystalline Phases of Poly(vinylidene fluoride) Films Prepared at Different Conditions. *J. Appl. Polym. Sci.* **2006**, *100*, 3272−3279.
(21) Frübing, P.; Wang, F.; Wegener, M. Relaxation Processes and Structural Transitions in Stretched Films of Polyvinylidene Fluoride and its Copolymer with Hexafluropropylene. *Appl. Phys. A: Mater. Sci. Process.* **2012**, *107*, 603−611.
(22) Nakagawa, K.; Ishida, Y. Annealing Effects in Poly(vinylidene Fluoride) as Revealed by Specific Volume Measurements, Differential Scanning Calorimetry, and Electron Microscopy. *J. Polym. Sci., Part B: Polym. Phys.* **1973**, *11*, 2153−2171.
(23) Gedde, U. W. *Polymer Physics,* 1st ed; Chapman and Hall: London, 1995.
(24) Gregorio, R.; Ueno, E. M. Effect of Crystalline Phase, Orientation, and Temperature on the Dielectric Properties of Poly(vinylidene fluoride) (PVDF). *J. Mater. Sci.* **1999**, *34*, 4489−4500.
(25) Kobayashi, M.; Tashiro, K.; Tadokoro, H. *Macromolecules* **1975**, *8*, 158−171.
(26) Bachmann, M. A.; Gordon, W. L.; Koenig, J. L.; Lando, J. B. *J. Appl. Phys.* **1979**, *50*, 6106−6112.
(27) Kochervinskii, V. V.; Malyshkina, I. A.; Markin, G. V.; Gavrilova, N. D.; Bessonova, N. P. Dielectric Relaxation in Vinylidene fluoride−hexafluoropropylene Copolymers. *J. Appl. Polym. Sci.* **2007**, *105*, 1101−1117.